Jiban Kumar Sarker (Bangladesh), Mehedi Ahmed Ansary (Bangladesh),
Md. Rezaul Islam (Bangladesh), A.M.M. Safiullah (Bangladesh)

Potential losses for Sylhet, Bangladesh in a repeat of the 1918 Srimangal earthquake

Abstract

A comprehensive earthquake loss assessment for the Sylhet City, Bangladesh was performed considering the 1918 Srimangal Earthquake (magnitude 7.6) as a scenario event. Primary objectives of this study were: (1) to generate credible earthquake losses to provide a baseline for coordination, capability development, training, and strategic planning for the planner and decision maker, and (2) to raise public awareness of the significant earthquake risk in the Sylhet City. Ground shaking, liquefaction, and earthquake-induced landslide hazards were characterized using region specific inputs on seismic source, path, and site effects, and ground motion numerical modeling. For the assessment of potential losses, a building inventory methodology and facilities for the Sylhet City was developed. For microzonation purpose 167 bore holes with SPT data were used. Also six shear-wave velocities at six locations were measured. For the assessment of loss, a building inventory methodology for the town of Sylhet was developed. 3040 buildings (12%) of the total were surveyed in the study area. On the other hand, for the vulnerability and potential loss assessment of water pipelines and gas pipelines system the water and gas delivery pipelines of the city were digitized into GIS.

From attenuation law, peak ground acceleration in the bedrock level was estimated and used to develop a regional combined seismic hazard map based on site amplification, liquefaction and landslide. These hazard maps were then overlaid and combined with the structural inventory maps and water and gas supply system maps, to produce maps of regional damage distributions. Combining the map of damage distributions with a map of population distributions for the area results in final regional estimates of direct monetary loss such as buildings, water and gas supply systems and non-monetary loss such as fatalities and injuries. The methods to combine the different hazards are based on weighted average approach. Finally economic loss estimation was estimated using the damages expected to be suffered due to the scenario event. The expected damage factor for buildings is 59%, maximum fatalities 7.0% at night and maximum injuries 8.3%. In case of lifeline, affected length for water pipe lines is 118.53 km and total number of damage points is 204 and affected length of gas supply system is 436 km and total number of damage points is 981.

The results of the loss assessment indicate that a future repeat of the 1918 Srimangal Earthquake would be catastrophic, resulting in possibly maximum 21674 deaths, more than 25875 injuries and a total economic loss of about US $219.25 million. Schools, hospitals, fire stations, ordinary buildings, and bridges will suffer significant damage due to the general lack of seismic design in the City. Lesser damage and losses will be sustained in the other earthquake scenarios although even the smallest event could result in significant losses.

Keywords: microzonation, site amplification, liquefaction, landslide, vulnerability.
JEL Classification: Q54.

Introduction

At 10 h 22 m 7 s (GMT) on 8 July 1918, one of the largest known earthquakes (Srimangal earthquake, magnitude 7.6) have occurred in the northeast region of Bangladesh. It damaged or destroyed the large majority of brick buildings, bridges, hospitals, water tanks, factories in the tea garden estates and killed 2 people (Sabri, 2001). Structural damage was widespread, extending as far as the whole area encompassing Sylhet, Moulavi Bazar, Habiganj, Brahmanbaria, Kishoreganj and Agartala (India). The shock was felt in a fairly large area at far east at Aijal (Monipur, India), west at Calcutta (West Bengal, India), south at Rangoon (Myanmar) and north at Katmundu (Nepal), an area of about 74000 sq. km was affected (Stuart, 1920). Large cracks, fissures and land slide was extensive in the epicentral area. One of the fissures was 150 mm length and 300 mm deep. Sand boils were observed in many places. The maximum Modified Mercalli (MM) intensity was VIII-IX (Sabri, 2001). Sylhet, which is now a rapidly growing urban area of Bangladesh, was subjected to strong ground shaking that resulted in many houses either being displaced off their foundations, settled differentially, or destroyed.

Obviously a repeat of the 1918 Srimangal Earthquake or even a smaller, moderate-sized event could be catastrophic to Bangladesh, particularly to the Sylhet city and surrounding areas. Based on seismic zoning map of Bangladesh (see Figure 1) and seismic hazards for Bangladesh (Sharfuddin, 2001), the Sylhet City is situated in the highest seismic zone.

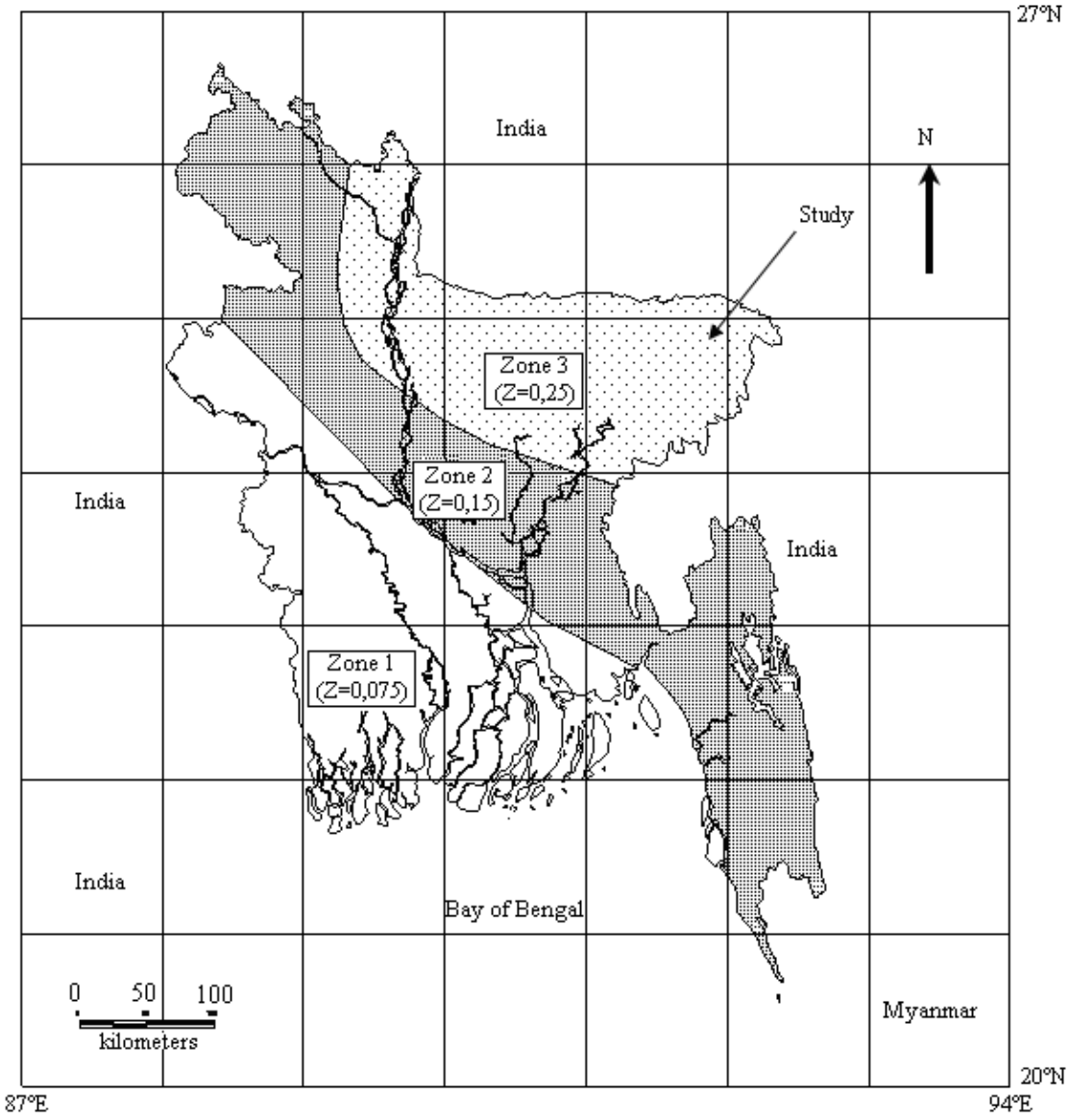

Fig.1. Seismic zoning map of Bangladesh (BNBC, 1993)

In this paper a comprehensive earthquake loss assessment of Sylhet City is presented. The purpose of the study was to evaluate the potential losses from 1918 Srimangal earthquake (M = 7.6) with the help of GIS. These results provided a basis for the city to effectively plan and prepare for future damaging earthquakes, and also a means to raise public awareness of the city's earthquake risk. A specific objective of the study was to estimate as accurately as possible the potential earthquake losses by: (1) characterizing the earthquake hazard input geologic, geotechnical, and seismological data; and (2) improving the inventory data. These efforts resulted in one of the most comprehensive estimations ever performed in Bangladesh.

1. Geology of the study area

The Sylhet Trough of northeastern Bangladesh is a tectonically complex province of the Bengal Basin (Figure 2). It comprises 12 to 16 km thick sequence of Late Mesozoic and Cenozoic age sedimentary rocks (Johnson and Alam, 1991). The Dauki fault system with huge vertical displacements represents the transition between the Sylhet Trough and the Shillong Plateau (Hiller and Elahi, 1988; Johnson and Alam, 1991).

The Sylhet Trough was developed due to contemporaneous interaction of two major tectonic movements: (1) uplift of the Shillong Massif in the north; and (2) westward propagation of the Indo-Burman mobile belt (Hiller and Elahi, 1988). Johnson and Alam (1991) argued that the Sylhet Trough had evolved from (1) a passive continental margin (pre-Oligocene) to (2) a foreland basin linked to the Indo-Burman Ranges (Oligocene and Miocene) and (3) a foreland basin linked to the south-directed overthrusting of the Shillong Plateau (Pliocene to Holocene).

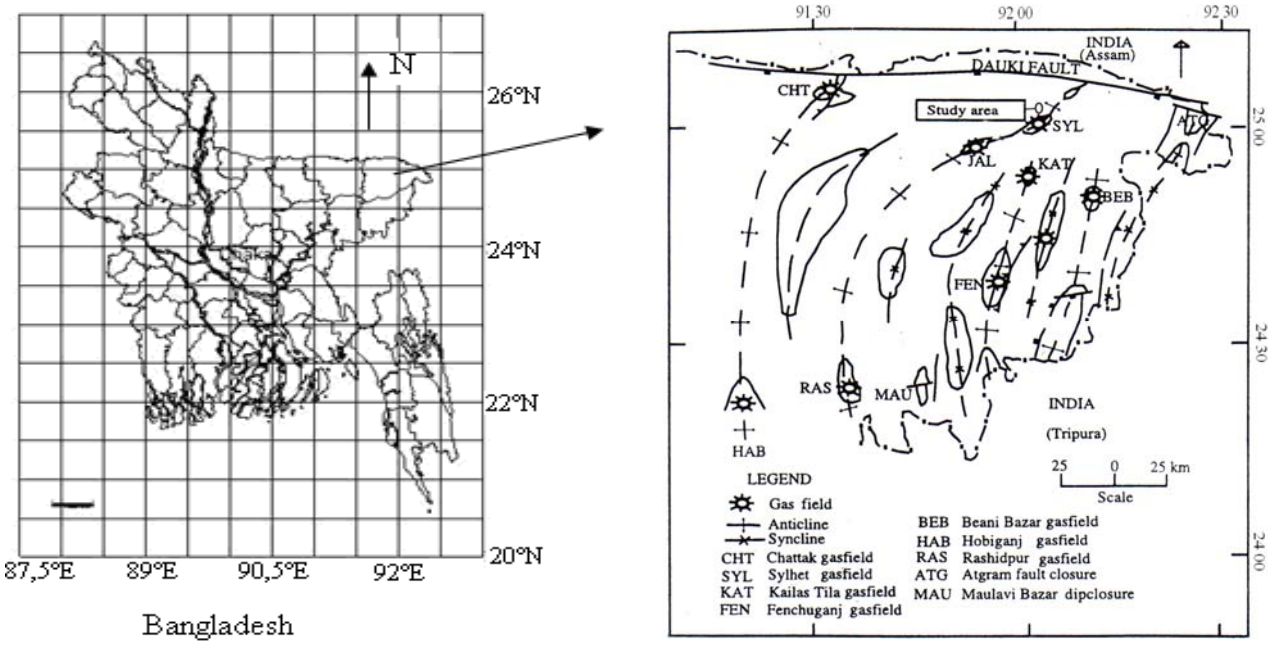

Fig. 2. Study area

The sedimentary sequence encountered in the formation of the structure is generally subdivided into the following lithostratigraphic units, from the oldest to the youngest: Bhuban (1194 m+) and Boka Bil (798 m) Formations of Surma Group (Miocene). Tipam Sandstone (646 m) and Girujan Clay (411m) Formations of Tipam Group (Mio-Pliocene) and Dupi Tila Formation (1095 m) (Plio-Pleistocene) (BAPEX, 1989).

The Surma Grup consists of a deltaic diachronous sequence of alternating sandstone, shale, sandy shale and siltstones (Brunschweiller, 1980). The fluvial Tipam Group is characterized predominantly by sandstones and sandy shale at the bottom and clay at the top. The major rock types of the Dupi Tila Formation are also fluviatile sandstone (Talukder et al., 2006).

2. Regional tectonics

According to Molnar and Tapponnier (1975), for the past 40 million years the Indian subcontinent has been pushing northward against the Eurasian plate at a rate of 5 cm/year, giving rise to the severest earthquakes and most known diverse land forms known. Recently, Bilham et al. (2001) pointed out that there was high possibility that a large earthquake may occur around the Himalayan region based on the difference between energy accumulations in this region. There is a seismic gap that is accumulating stress, and a large earthquake may occur someday when the stress is relieved. A recent study by OIC (2009), identified five earthquake sources for Bangladesh as shown in Figure 3.

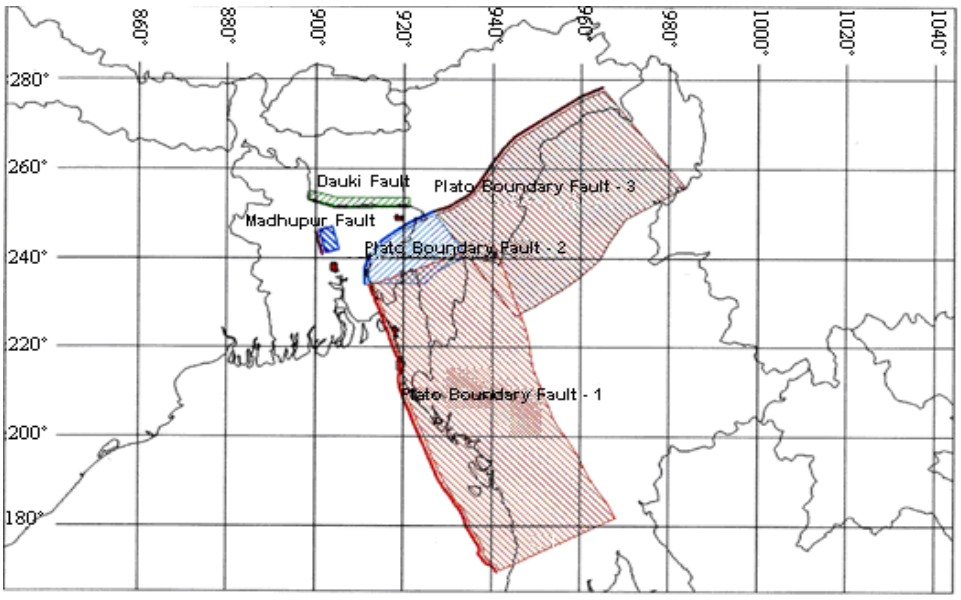

Fig. 3. Scenario of Earthquake fault model (OIC, 2009)

The major past earthquakes and some recent earthquakes that affected Sylhet are presented in Table 1.

Table 1. Some historical earthquakes with magnitude, intensities, epicentral distance and focal depth

Name of past earthquake	Fault	Magnitude	EMS intensity	Distance (km)	Focal depth (km)
1869 Cachar earthquake	Plate Boundary 2	7.5	VIII	92	56
1885 Bengal earthquake	Modhupur	7.0	V	234	72
1897 Great Indian earthquake	Dauki	8.1	IX	151	60
1918 Srimangal earthquake	Plate Boundary 2	7.6	IX	71	14

3. Inventory data

3.1. General. Recently Sylhet City Corporation office divided this municipality area into 27 wards on the basis of voter list. The Sylhet City Corporation authority did not prepare updated map containing 27 wards. A paper map was collected from Sylhet City Corporation office and based on GPS value of different fringes location as well as nucleus location of the town, the map was digitized using MapInfo Software.

In this study Microsoft Access and Excel Software and GIS Map Info Professional have been used to develop a relational database to store and analyze soil data and building data. The format of the data collection questionnaire used in the survey is similar to FEMA (Federal Emergency Management Agency).

3.2. Population of the study area. In census 1991 population was given according to local area so by investigating this scenario together with ward list containing individual area is given. Population distribution is also determined according to ward map where 27 wards are distinguished. According to the census 1991 of the population of the study area was 234355. Considering the growth rate since 1961 to 1991 and based on the 1991 base population for the municipal area, it is estimated that the population of 2003 for the same area would be around 311050. During 1991 annual population growth was 3.36%. For interpolating the population of 2003 this annual growth rate is assumed. In 1991 household size in the urban area was 6.4 and the household size for study area 6 is assumed.

The increase of population in Sylhet City is largely due to the migration, which was 56% of the total increase in the city during 1974-81. The increase has been higher in the rural-urban fringe areas than in the inner city areas.

Construction sub-sector has also expanded in recent years, with a boom in luxury residential housing and shopping centers. This is largely due to the remittances of Sylhetees living in the UK. Population density map is shown in Figure 4.

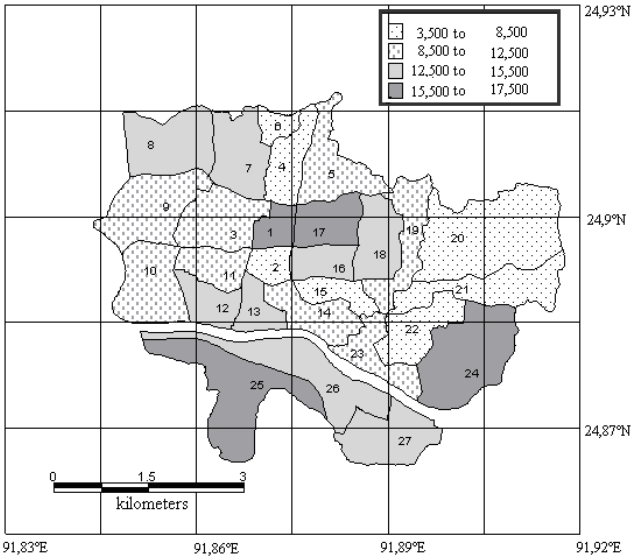

Fig. 4. Population density map of Sylhet City Corporation

3.3. Land use. Of the total area of municipality, about two thirds are built-up while agricultural land, vacant space and water bodies take up another one-third. Residential use takes more than 50% of the land while commercial use takes about 5%, educational and health together about 5%, administration takes 2.5%, and industrial takes only over 1%. Other uses take small proportions of land. At present the most conspicuous developments are taking place in he form of luxury and expensive residential buildings and shopping centers.

Building stock data from census reports was gener-

ally compiled at district level, but for big cities like Sylhet, ward level data exist (BBS, 2001). For this study, ward was adopted as the basic geographical reference (geo-code) for the loss model.

3.4. Soil data used. A total 271 boreholes with SPT data were collected from different relevant organizations and stored in Microsoft Excel. Majority of the borings were drilled up to a depth of 15 m to 18 m. Among these, 9 boreholes with SPT-N data up to a depth of 30 m were directly collected by BUET (Bangladesh University of Engineering and Technology) for checking the authenticity of other collected data. The typical available boring is up to a depth of 15 m.

Collected boreholes from Sylhet City Corporation area were located in the digitized map based on GPS value of each borehole (Islam, 2005). Figure 5 shows borehole locations together with the ward map.

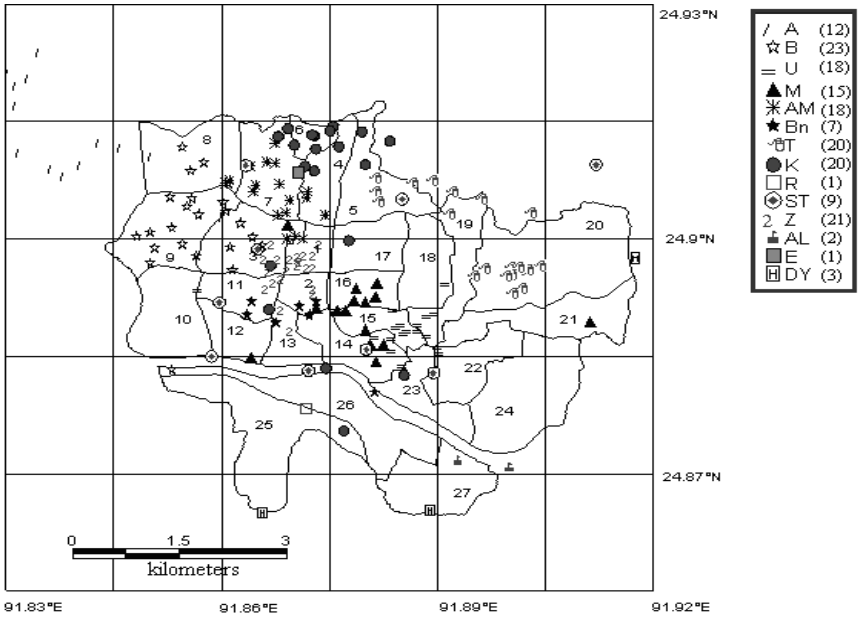

Fig. 5. Borehole location map considered for this study

3.4.1. Hillocks data. The eroded hills are mainly formed by the hill ranges and hillocks (locally called tila) appearing in the north-east and south of Greater Sylhet and also around the Sylhet town. These hill ranges attain a low elevation and have a gentle slope. Hillocks are scattered in Sylhet City Corporation area. Among 27 wards some northern out fringe wards such as 5, 7, 8 have some hillocks and some core wards such as 1, 9, 10, 11, 17, 18, 19, 20 have some hillocks. Figure 6 shows location of hillocks.

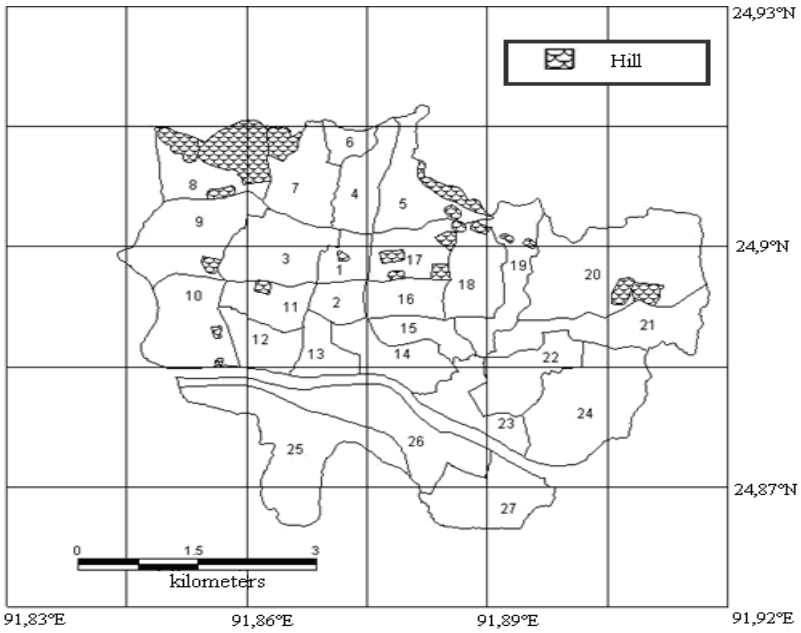

Fig. 6. Hill location map in Sylhet City Corporation

3.4.2. Building data. The building stock of Sylhet Municipality exhibits a mix of several different building technologies. The most commonly used building categories are:

1. Reinforced-concrete frame building with partition wall.
2. Brick masonry buildings with reinforced concrete roofs and using cement mortar.
3. Informal brick masonry buildings (which may or may not use cement mortar).
4. Buildings made of other materials such as tin sheets, thatch, mud, wood and other lightweight elements.

The first two categories typically constitute engineered constructions in which the assistance of qualified engineers is usually taken at each stage. The last two categories are non-engineered constructions, wherein the services of skilled engineers may not have been employed.

A sample sites survey of the area is important for building damage estimation due to earthquakes, and also for earthquake disaster risk management. In the following paragraphs a pilot study undertaken for this survey was elaborated.

3.5. Methodology sample site survey. The methodology adopted for the sample site survey consisted of several tasks that are described briefly in below.

3.6. Selection of sample sites. For survey purpose 27 wards have been divided into four types. Group 1, which clustered 4, 5, 6, 7, 8, 9, 19. Ward 7 is comprehensively surveyed. Group 2 in which wards 1, 2, 3, 11, 15, 16, 17, 18 among which all wards are partially surveyed. 10, 12, 13, 14, 23 wards are included in groups 3 where wards 12, 13, 14 are partially surveyed. Group 4, which is clustered with wards 20, 21, 24, 25, 26, 27 where no survey is conducted but data is collected from BBS (1991). Figure 7 shows location of these surveyed wards with respect to Sylhet.

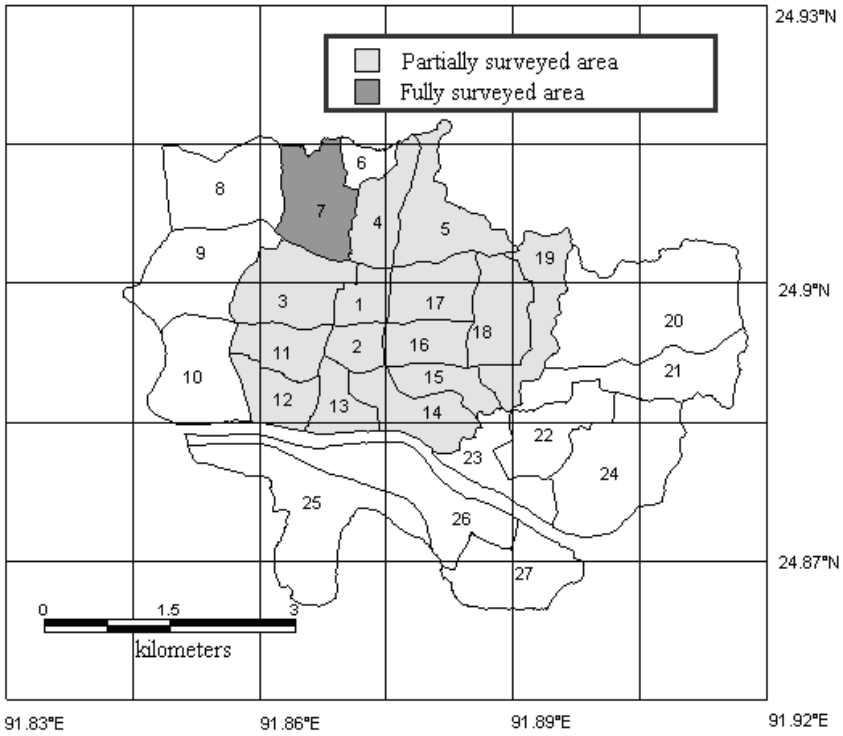

Fig. 7. Location map of sample sites

3.7. Survey format design and generation. A survey format was developed for the conduction of the pilot study survey. The format allowed for recording information from:

1. A structured interview with the house owner.
2. Visual observation of the condition of the buildings.
3. Measurement of the geometry of the sample building with tape.

For the pilot study, interview was adopted and questionnaire format was developed.

The questions for the interview consisted of about 40 to 50 queries to clarify in detail the characteristics of the buildings.

The survey format consisted of three parts: general information, building details, and lifeline details.

3.8. Results of the site survey. Since Sylhet is an old city, several engineered constructions are also very old and were constructed decades ago. These buildings have already exceeded their useful service life and several of them have deteriorated badly. Most buildings that are found in Sylhet are non-

engineered. These structures are typically designed and constructed by people without appropriate technical qualifications. Most such buildings are designed without any detailed analysis and may also be of a poor quality. Lifeline facilities distributed over the city area. But proper planning and design for earthquake resistance have not been considered.

3.8.1. Building typology and classification. The sample site survey results helped to classify all buildings in Sylhet into six types based on their definition in European Macroseismic Scale (Grunthal, 1998).

3040 buildings (only 12% of the total) were surveyed from the above-mentioned wards. The building survey results together with wall and roof material as described in BBS, are used to understand the building type distribution pattern. The results of the total building survey are summarized and presented in Table 2.

Table 2. Building classification according to survey results and BBS (1996)

Ward No	Housing unit	EMSA	EMSB1	EMSB2	EMSC	EMSD	EMSF
1	1399	0	512	92	675	9	111
2	700	0	256	46	338	4	56
3	1022	0	374	67	492	6	83
4	335	2	137	3	169	1	23
5	980	5	400	8	496	2	69
6	702	4	287	6	355	2	48
7	1238	6	506	10	626	3	87
8	1157	6	473	10	585	3	80
9	780	4	319	6	394	2	55
10	926	114	321	29	214	3	245
11	715	0	262	47	345	4	57
12	1170	143	405	37	271	3	311
13	1061	130	368	33	246	3	281
14	1024	126	355	32	237	3	271
15	567	0	208	37	273	3	46
16	1147	0	420	75	553	7	92
17	1380	0	505	91	665	8	111
18	1287	0	471	85	621	7	103
19	858	4	351	7	433	2	61
20	670	82	232	3	174	1	178
21	608	75	211	3	158	1	160
22	317	0	116	21	153	2	25
23	919	113	318	29	213	3	243
24	1448	178	502	6	376	2	384
25	1425	175	494	6	371	2	377
26	1058	130	367	4	275	2	280
27	1099	135	381	5	286	2	290

3.8.2. Construction age of buildings. Of the 3040 building samples (Figure 8) it is appeared from the building survey that more than 62% of the buildings in Sylhet City Corporation area are less than 11 years old. However, about 4% of the buildings in Sylhet City Corporation area are more than 40 years old indicating to a higher vulnerability, especially if one considers that the predominant type of older buildings is of type EMSB. There are significant growths in EMSC constructions using RCC beam and column started only 20 or 30 years ago. Although some of these buildings are made of RCC, they are basically non-engineered and are extremely vulnerable.

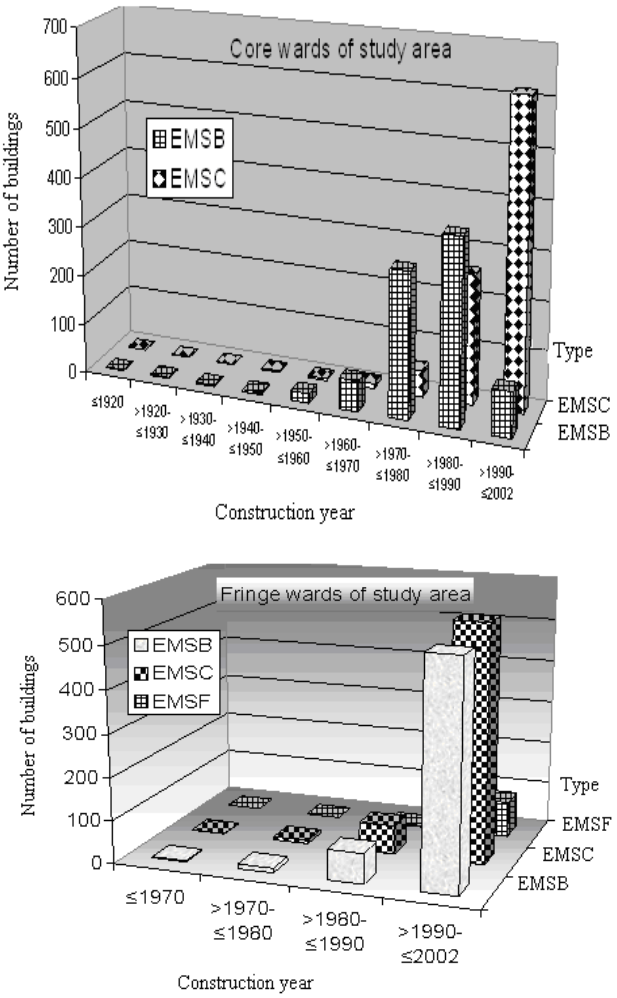

Fig. 8. Distribution of buildings types with construction year for core and fringe ward in the study area

3.8.3. Number of stories and building area. A majority of buildings include ward number 4, 5, 6, 7, 8, 9, 10, 20, 21, 24, 25, 26, 27 posses; more than 85% of buildings are 1-storied and the rest of buildings about 15% are 2-5 stories high, on the other hand, include ward number 1, 2, 3, 11, 12, 13, 14, 15, 16, 17, 18, 19, 22, 23 posses; more than 49% of buildings are single-storied and the rest about 51% are 2-7 stories high. Figure 9 shows the distribution of buildings in the areas according to number of stories and floor space. In the study area, for seismic loss estimation for building damage it is needed to know the average weighted house area as well as average weighted floor space.

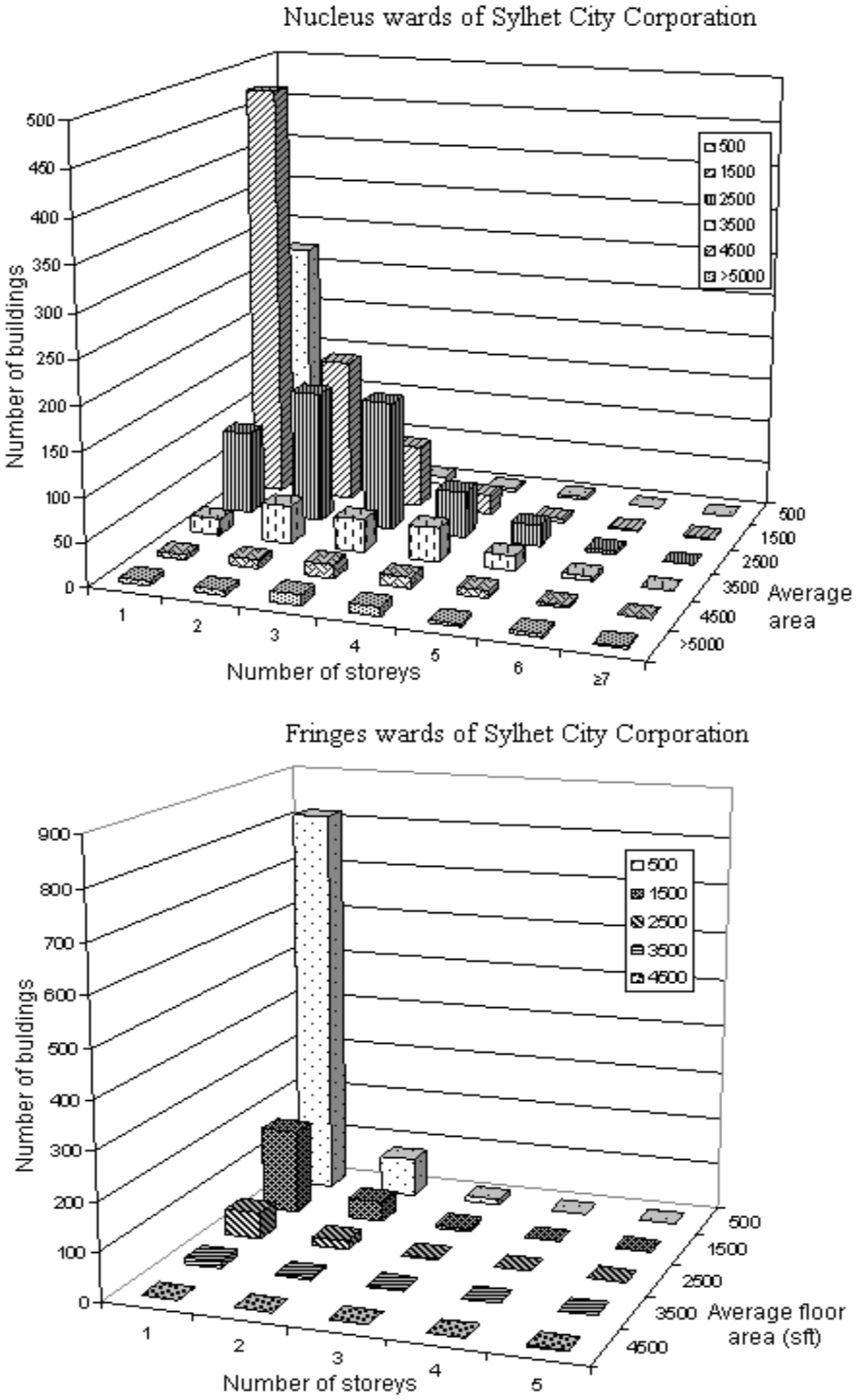

Fig. 9. Distribution of building types according to their storey and floor area for core and fringe wards of the study area

3.9. Lifeline data. Lifelines include water and sewage systems, electric power and communication systems, natural gas facilities (including pipelines), transportation systems, airports, and harbor facilities. In this study for the analysis of potential losses of lifelines only the most up-to-date site-specific data for water supply system and natural gas supply system were collected and analyzed using Cheng et al.'s (2002) method.

3.10. Water supply pipelines. The construction blueprints of water delivery pipelines (prepared by LGRD: Local Government and Rural Development) of the study area were digitized into a Geographical Information System (GIS) for analysis and assessment. Water pipe line and other features of the study area are shown in Figure 10. Pipeline distribution according material and diameter is also shown in Figure 11a and Figure 11b. From the collected data it can be seen that only the municipality is well served by water mains where 28.8% of the households have access to piped water.

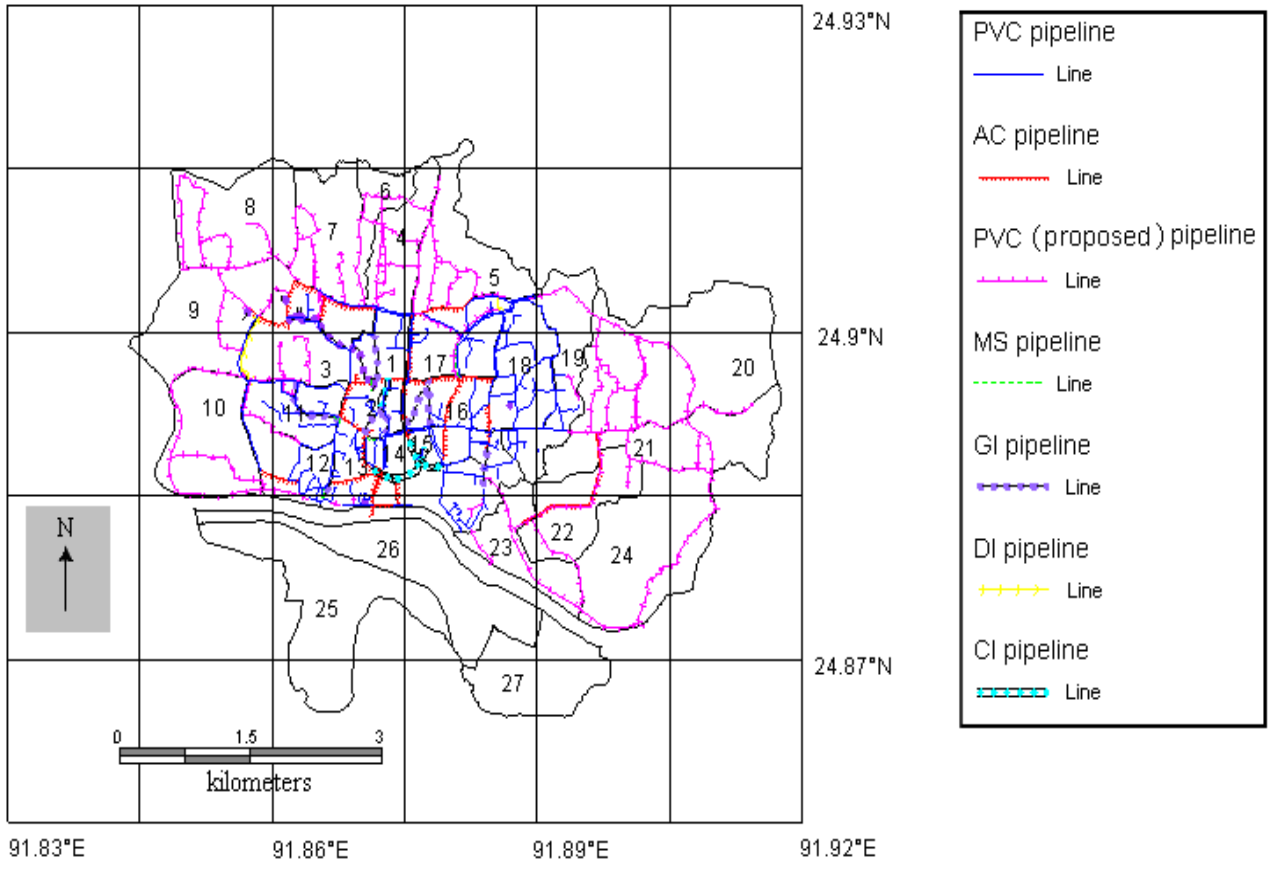

Fig. 10. Map showing distribution of water pipelines according to material of Sylhet City

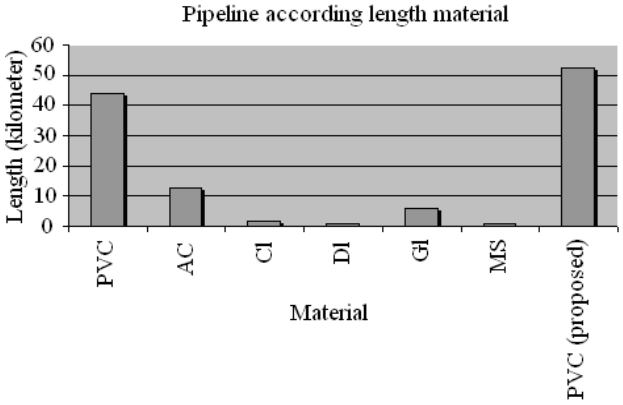

Fig. 11a. Distribution of lengths of water pipelines according to material in the study area

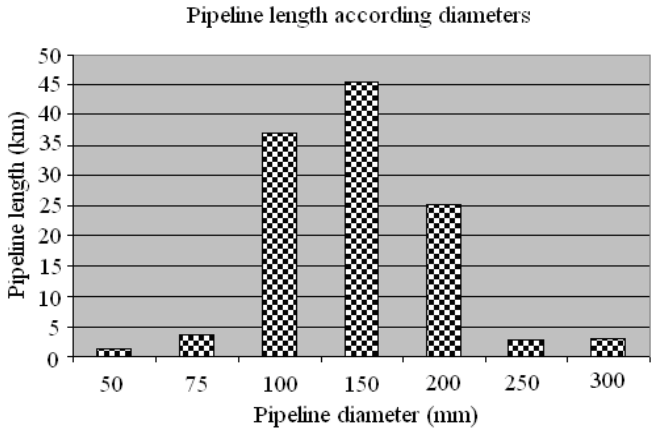

Fig. 11b. Distribution of lengths of water pipelines according to diameter in the study area

4. Natural gas pipelines

The construction blueprints of natural gas supply system (prepared by Jalalabad Gas Office, 2005, Sylhet) of the study area were digitized into a Geographical Information System (GIS) for analysis and assessment. In order to perform analysis, the pipelines were divided into two groups according to their diameters and the study area is divided into 1km × 1km grid with pipelines enclosed in the grid. Gas pipelines distribution of the study area are shown in Figure 12. Pipeline distribution according to material and diameter is also shown in Table 13.

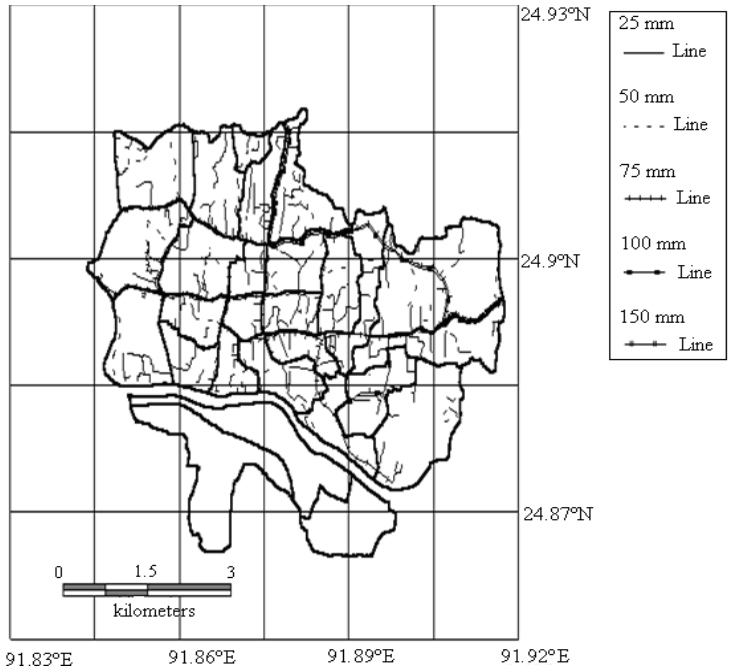

Fig. 12. Gas pipeline distribution according to diameter

4.1. Inventory overview. Sylhet City has an area greater than 42.8 km^2 with about 51831 households in the city and a total population of about 311050 people. The 2003 population density distribution is shown in Figure 4 and total number of building in the city is 25992. Major portion of the building is associated with residential housing.

The Sylhet municipal water supply system has a capacity of more than 36,37,000 litres per day. The length of pipeline installed exceeded 118 km. The piped water system in Sylhet city serves about 3871 domestic connections and 156 commercial as well as industrial connections by Pourashava (Sylhet City Corporation, 1998). The Sylhet municipal Gas supply system has a capacity of more than 144.9 km but the length of pipeline installed exceeded 106.44 km. In the total pipelines there is a total number of 85 gas valve stations.

5. Assessment of seismic hazard

The methodology provided in HAZUS is a post earthquake management model that can be applied in regions that are at risk for earthquake disaster. The methodology generates estimates of the consequences to a city or region due to a scenario earthquake. Scenario earthquake could be a specified earthquake with magnitude and location. The evaluation methodology consists of three basic steps (Schneider and Schauer, 2005):

1. Study region definition: definition of the region, selection of the application area, selection of the appropriate data from the earthquakes.
2. Hazard characterization: definition of the earthquake hazard, hazard type and source, fault type, earthquake location.
3. Damage and loss estimation: social and economic loss estimation, structural hazard estimation.

HAZUS, as a risk assessment model, can address the earthquake hazard in the US. It was developed over 17 years in the US. It is a state-of-art decision support tool for assessing disasters. It is the first PC-GIS based evaluation tool. Capabilities in HAZUS include earthquake, flood and hurricane hazard characterization, building, essential facilities damage analysis, computing direct economic losses and secondary hazard.

However, as it is, HAZUS is not ready for use in Bangladesh. National and district boundaries and characterization of the earthquake data used in HAZUS are currently only available for the US. HAZUS can provide a starting point for the development of a disaster risk assessment tool which could be used in Bangladesh considering user requirements and data availability. Earthquake disaster risk assessment and evaluation for Turkey was done successfully by Korkmaz (2009).

Figure 13 presents the flowchart for this study. In the regional seismic loss estimation analysis, it is needed to determine the bedrock motion in the region. The most common method involves the use of an empirical attenuation relationship. These relationships express a given ground motion parameter in a region as function of the size and location of an earthquake event. Applying statistical regression analyses to recorded data numerous relationships in the past was developed. Often these relationships were developed with different functional forms and with different definitions of

ground motion, magnitude, distance, and site conditions. To select the most suitable attenuation law for predicting rock motions, 1885 Bengal earthquake, 1897 Great Indian earthquake and 1918 Srimangal earthquake were considered. The requirements for selecting the attenuation law are as follows:

1. Applicable to the ground condition of engineering bedrock in this study.
2. Able to explain the observed or analyzed earthquake motion of 1885 Bengal earthquake, 1897 Great Indian Earthquake and 1918 Srimangal earthquake.

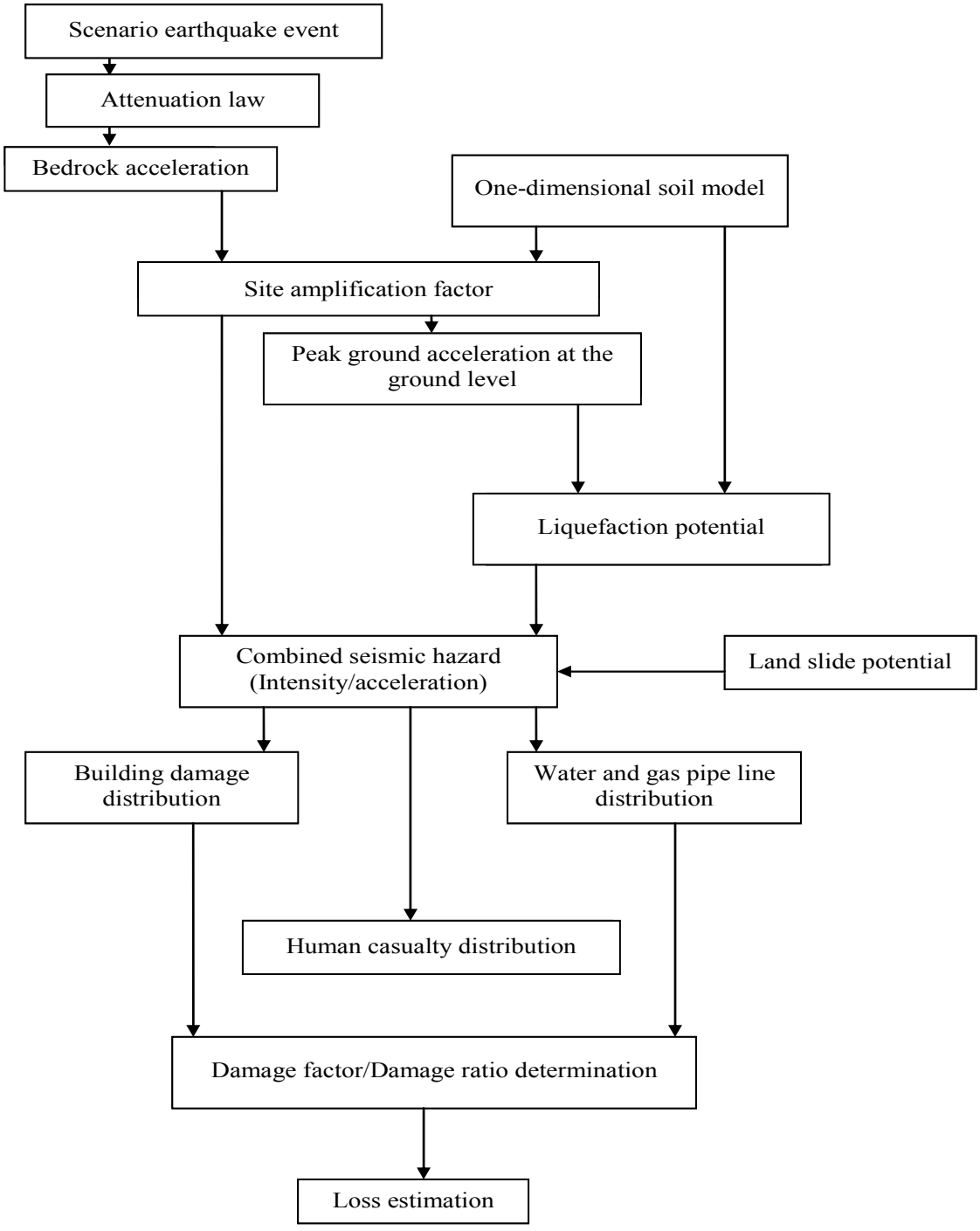

Fig. 13. Flowchart for the study

In this study, the engineering bedrock was assumed to be the layer at which the shear wave velocity (V_s) exceeds 350 m/s, which exist almost 30 m deep from the surface of the study area. The shear wave velocity was estimated by using equation of Tamura and Yamazaki (2002). Also, direct shear wave velocity was measured at six locations. Distance versus PGA values for earthquakes was plotted on log-log paper. From isoseismal maps, the epicentral distances of different locations and their intensities are found (see Figure 14).

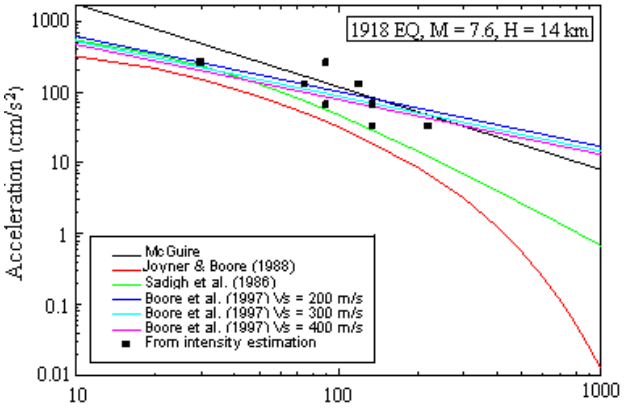

Fig. 14. Distance versus PGA values for 1918 Srimangal earthquake

These intensities were converted into PGA by the following Trifunac and Brady (1975) equation:

$$log\ (PGA) = 0.014 + 0.3\ (MMI). \quad (1)$$

From these plots (Figure 17), it was found that McGuire (1978) equation:

$$PGA = 0.0306e^{0.89M}r^{-1.17}e^{-.2}\ cm/s^2,$$

where M is magnitude and r is hypocentral distance, as well as Boore et al. (1997) equations follows the PGA trend. Since, McGuire equation was already used for Bangladesh for seismic hazard analysis (Sharfuddin, 2001) and due to its simple form; it is selected for further use. Table 3 presents the PGA values at bedrock level from different attenuation laws for different scenario event. Finally, 1918 Srimangal earthquake (M = 7.6) with the highest PGA value 0.18g (where g is the gravitational acceleration) at bedrock eslevel was selected for Sylhet.

Table 3. PGA values at bedrock level from different attenuation laws for different scenario event

Attenuation law	PGA for Cachar earthquake (1869)	PGA for Great Indian earthquake (1897)	PGA for Srimangal earthquake (1918)
McGuire (1978)	0.12g	0.10g	0.18g
Sadigh et al. (1986)	0.0106g	0.0328g	0.0238g
Joyner and Boore (1988)	0.0078g	0.0108g	0.0163g
Boore et al. (1997)	0.030g	0.017g	0.055g

6. Site amplification analysis

Site amplification of earthquake motion is one of the most difficult site effects to model. The difficulties result from: (a) the lack of sufficient data on local soil parameters; (b) the lack of sufficient strong ground motion at locations with different surface soil types; (c) the lack of sufficient strong ground motion data from vertical array measurements; (d) the inability to accurately quantify the non-linear characteristics of soil; and (e) the use of approximate models to represent the true non-linear behavior of soils when subjected to dynamic forces (Kiremidjian et al., 1991).

Numerous methodologies were proposed for estimating the surface ground motion from the motion at the bedrock level and the geologic characteristics of local soil conditions. Current methods for estimating ground motion site amplification can generally be divided into three types: (a) empirical multiplication factors; (b) theoretical transfer function models; and (c) dynamic non-linear models. For estimating ground motion site amplification, a lot of researchers used different methods. The most commonly used transfer function model is included in the computer program SHAKE developed by Schnabel et al. (1972). Vibration characteristics at different points of the study area were estimated by employing one dimensional wave propagation program SHAKE. SHAKE discretizes the soil profile into several layers and uses an iterative technique to represent the non-linear behavior of the soil by adjusting the material properties at each iteration step. The required input information includes depth, shear wave velocity, damping factor and unit weight of each soil layer.

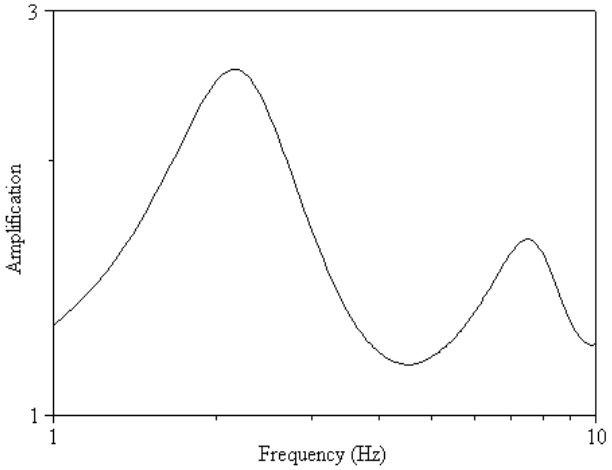

Fig. 15. Typical amplitude-frequency

The computations were made in the frequency range of 0 to 20 Hz at frequencies of every 0.05 Hz interval. The loss of energy of seismic waves in the soil layers is also considered. An estimation of the fundamental frequency and the maximum value of the amplification were obtained at each site. Figure 15 shows a typical amplitude-frequency curve of the study area. Amplification factors were calculated as a function of site response category, spectral frequency, soil thickness, and input rock motion. Considering the highest PGA value 0.18g (where g is the gravitational acceleration) at bedrock level the resulting mapped peak horizontal accelerations based on the amplification at ground urface varied between 0.35g to 0.45g in the Sylhet City (Islam, 2005) (see Figure 16).

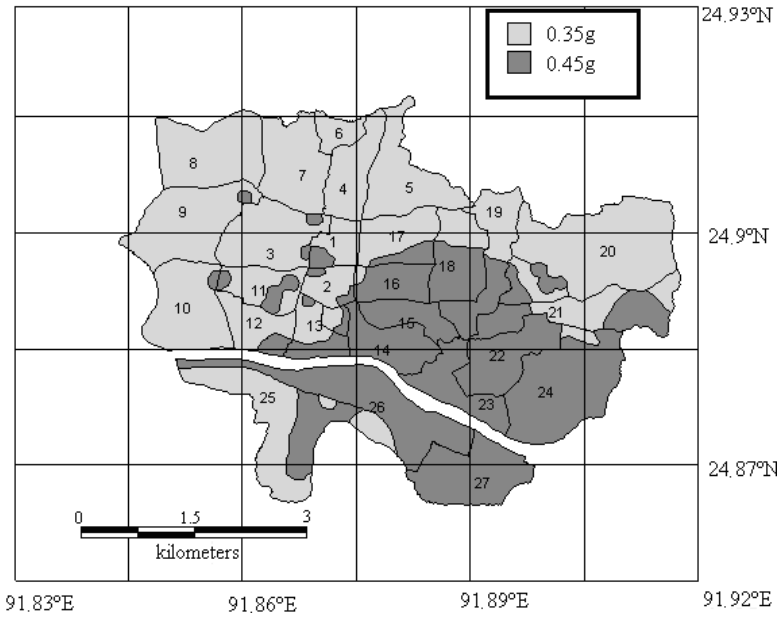

Fig. 16. Map showing regional distribution of peak ground acceleration in Sylhet City Corporation

6.1. Liquefaction analysis. Regional liquefaction hazard mapping is typically done using either a geologic or a geotechnical technique (Juang and Elton, 1991). During the past 25 years, several geotechnical techniques for analyzing soil liquefaction were proposed, resulting from the need for a more quantitative estimate of regional liquefaction hazard. Most of these techniques involve the comparison of the cyclic stress ratio generated by an earthquake with the cyclic stress ratio which would be required to liquefy the soil (Youd, 1991). The most commonly applied technique was developed by Seed and Idriss (1971). According to their method, the cyclic stress ratio generated by the earthquake (*CSRE*) at a particular depth below ground surface is computed as follows:

$$CSRE = \tau_{av}/\sigma'_o = 0.65(a_{max}/g)(\sigma_o/\sigma'_o)\, r_d\,, \qquad (2)$$

where, a_{max} is equal to *PGA* at the ground surface (in % of *g*), *g* is the acceleration due to gravity (in *g*), σ_o is the total overburden stress in the soil at the depth in question, σ'_o is effective overburden pressure, r_d is the depth-dependent stress reduction factor.

The cyclic stress ratio required to induce liquefaction of the soil (*CSRL*) is determined from empirical charts relating *CSRL* to corrected penetration resistance, $(N_1)_{60}$, calculated from standard penetration test (SPT) values as:

$$(N_1)_{60} = C_n\,(ER_m / 60)N_m\,, \qquad (3)$$

where, ER_m is equal to the SPT measured potential energy value, C_n is equal to σ'_o – dependent correction factor, N_m is the measured SPT resistance value.

The empirical charts estimate the *CSRL* needed to induce soil liquefaction for a given magnitude and $(N_1)_{60}$ value. The *CSRE* at the soil site due to the given magnitude earthquake was calculated by equation (2). If the computed *CSRE* is equal to or greater than the *CSRL* then liquefaction is assumed to occur at the site for the given earthquake.

A more recently developed geotechnical method for evaluating soil liquefaction was proposed by Iwasaki et al. (1982). This method is similar to Seed and Idriss (1971) method described above in that it also involves the calculation of a stress ratio giving a "yes" or "no" answer for the occurrence of liquefaction, but the Iwasaki et al. (1982) method goes one step further by attempting to quantify the severity of the liquefaction. The stress ratio or liquefaction resistance factor, F_L is defined as:

$$F_L = R/L, \qquad (4)$$

where *R* is the soil liquefaction capacity factor, *L* is the dynamic load induced in the soil by the seismic motion.

R is assumed to be a function of the *SPT* value and the effective overburden pressure in the soil and is calculated from equations for different ranges of mean grain size, D_{50}. The equation for calculating *L* is almost identical to that given for *CSRE* in equation (2). The severity of liquefaction is quantified with a liquefaction potential index, P_L, defined as:

$$P_L = \int_0^{20} F(z)\,w(z)\,d(z), \qquad (5)$$

where $F(z) = (1\text{-}F_L)$ for $F_L \le 1.0$, $F(z)$ = for $F_L >$ 1.0, $W(z) = (10 - 0.5\,z)$ for $z \le 20$ m, $W(z) = 0$ for $z > 20$ m, $P_L > 15$ very high possibility of liquefaction, $15 > P_L > 5$ high possibility of liquefaction, $5 > P_L > 0$ low possibility of liquefaction, $P_L = 0$ very low possibility of liquefaction.

The value of liquefaction potential, P_L indicates that a soil mass is susceptible to liquefaction if $P_L > 0$. If the value of P_L is large, the soil is very susceptible for liquefaction. Using the above methods, the liquefaction resistance factor, F_L, for the top 20 m of soil, and the resulting liquefaction potential, P_L for the 271 sites were calculated. Result of Liquefaction potential has been presented in Figure 17.

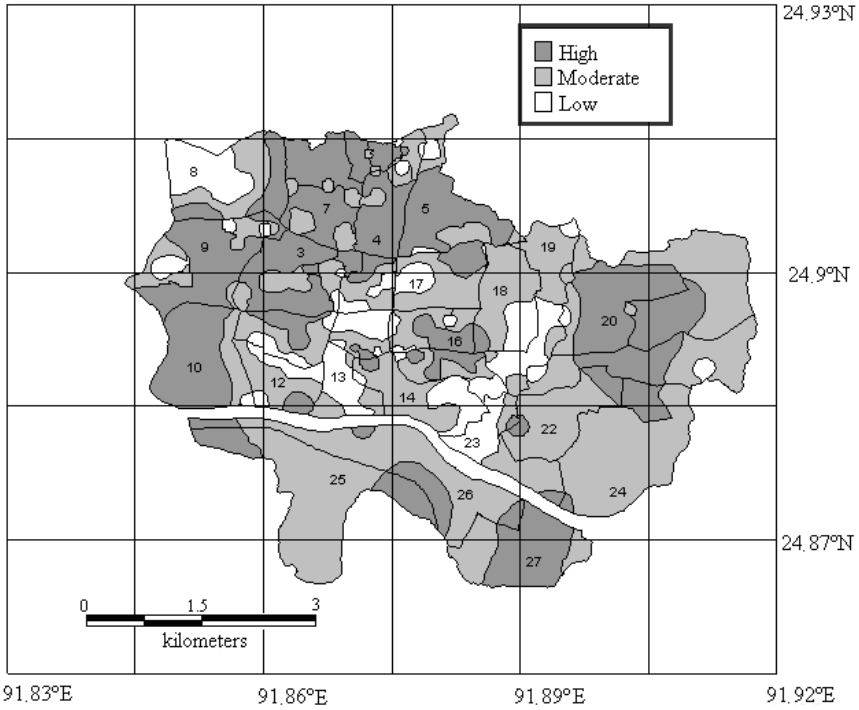

Fig. 17. Map showing regional distribution of liquefaction

6.2. Landslide analysis. The effects of earthquake-induced landslide have received much less research attention than the seismic effects of soil amplification and liquefaction discussed in the previous Sections. In addition to the movement associated with liquefaction-induced settlement and lateral flow, there is also a potential for landslides in sloping terrain, where the additional seismic forces may temporarily exceed the slope strength. Landslide hazard is typically very difficult to quantify because landslides come in many forms and are caused by a variety of processes. The local site factors that affect landslides generally include slope stability, geology, slope angle, hydrological conditions, vegetation, land use, and severity of the earthquake. Most of these factors are necessary for the investigation of an individual slope, but for seismically-induced landslide analysis on a broad regional basis, the factors are typically limited to slope angle, geology, location of previous landslides, magnitude of the seismic event, and distance from the source (Hansen and Franks, 1991).

As with liquefaction regional landslide hazard has traditionally been analyzed in a qualitative manner utilizing expert opinion, although recently more quantitative geotechnical methods have been proposed. The qualitative methods typically produce microzone maps indicating the relative susceptibility of various regions to landslides with no investigation into the possible triggering mechanisms for the land movement. The maps often result from an expert analysis of regional factors such as previous landslide locations, geologic deposits, and topography.

The complicated nature of the landslide process has made regional estimates of this local site effect very difficult to define quantitatively. Most of the recent research in this field has focused on determining the critical level of a given ground motion parameter that will trigger landslides in various geologic deposits. Wieczorek et al. (1985) model a landslide as a transnational failure on an infinite slope with a depth of 3 meters. They define three classes of geological units, assign shear parameters for each class, and then perform stability analyses using dry and saturated conditions to obtain the static factor of safety (*FS*) for each class. Based on the static *FS*, the critical acceleration to begin the process of slope failure is computed as:

$$a_c = (FS - 1)g \sin\theta, \quad (6)$$

where: θ is the slope angle, *FS* is the factor of safety determined from a static slope stability analysis, *g* is the acceleration of gravity.

Several recorded strong ground motions were analyzed to develop average curves of induced landslide displacement versus a_c. The critical levels of

displacement to produce structural damage are identified, such as 100 mm for cohesive slides (Wilson and Keefer, 1985). The a_c values that correspond to these assumed critical displacement values are determined from the displacement vs. acceleration curves. These a_c values are compared to the regional estimates of surface peak ground acceleration to give a prediction for the occurrence of damaging earthquake-induced landslides in the area. Based on available information stability analysis was performed as by Wieczorek et al. (1985) and using GIS a landslide hazard map is presented in Figure 18.

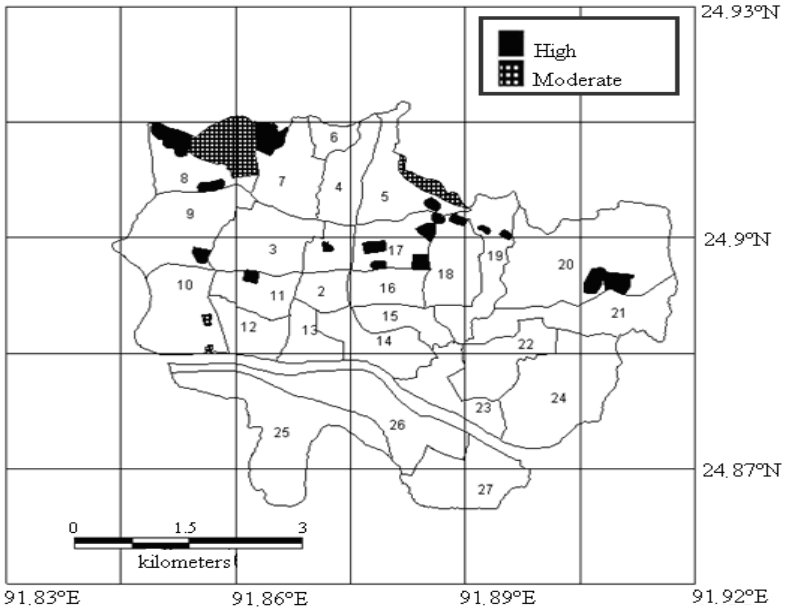

Fig. 18. Landslide potential map

6.3. Combination of ground shaking hazard, liquefaction and landslide. Ground shaking hazard and hazards due to secondary site effects are combined on the basis of experts' opinion (Kiremidjian, 1992). The intensities of combined hazard map were estimated and distributed over the ward map. The intensities lie between 8 to 11 (0.34g to 1.56g). 5.5% of the total area may suffer intensity 8 (0.34g), 28% may suffer intensity 9 (0.53g), 65% may suffer intensity 10 (1.05g) and only 1.5% of the total area may suffer intensity 11 (1.56g). The combined intensity (i.e., the combined hazard map) is shown in Figure 19.

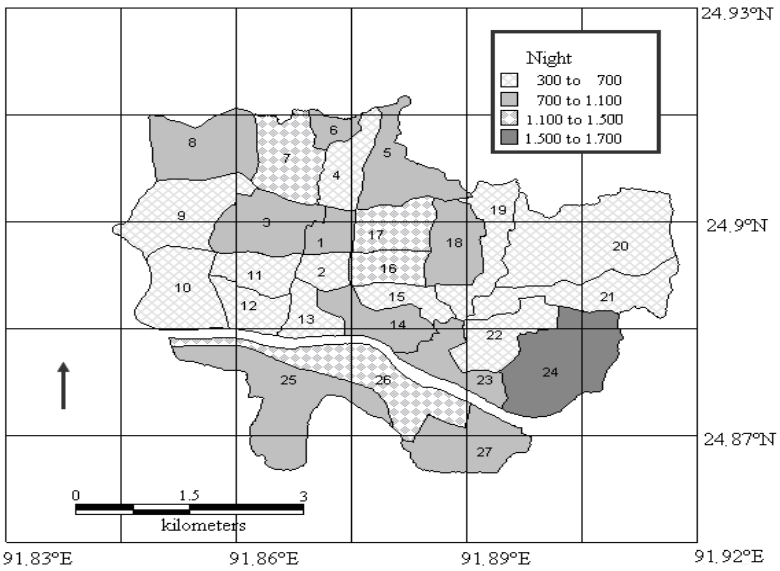

Fig. 19. Map showing regional distribution of combined seismic peak ground acceleration in the study area (after Islam, 2005)

7. Assessment of seismic damage

7.1. Damage distributions. Methods for estimating regional distributions of earthquake damage to buildings, bridges, dams, utility systems, and otherman-made structures have been the subject of extensive research over the past several decades (Rojahn, 1993). Reitherman (1985) provides a detailed review

of over thirty earthquake damage estimation methods. Damage assessment for a region typically depends upon three factors:

1. The level of seismic hazard in the region, including the effects of local site conditions.
2. The distribution of facilities in the region, according to earthquake engineering class.
3. The definition of functions that relate the expected levels of damage for the various earthquake engineering classes to the estimated levels of seismic hazard.

There are several definitions for damage and also several relationships for estimating damage due to given levels of seismic hazard for various facility types.

As in Japan and the United States, Bangladesh's earthquake assessment studies have commenced. In the US, several methodologies and standards such as HAZUS (developed by FEMA) and Applied Technology Council (ATC) 13-20-21 and 126, provide comprehensive earthquake loss estimation methodology for post-earthquake assessment.

Fragility curves are used in the FEMA/NIBS methodology to estimate damage to buildings resulting from ground shaking (Whitman et al., 1997). The fragility curves predict the probability of reaching or exceeding specific damage states for a given level of peak earthquake response. The probability of being in a particular state of damage, the input used to predict the building related losses, is calculated as the differences between fragility curves.

Building of the fragility curves are log-normal functions that describe the probability of reaching or exceeding structural and non-structural damage states, given deterministic estimates of spectral responses, for example, spectral displacement. These curves take into account the variability and uncertainty associated with capacity curves properties, damage states and ground shaking.

Fragility curves are used for estimation of damages of buildings in particular area. A number of fragility curves exist for Indian Buildings prepared by Arya (2000) and for Nepalese buildings prepared by Bothara et al. (2000). There also exist a number of fragility curves for different types of structure and for different earthquake intensities (Kircher et al., 1997; Fah et al. 2001; Yamazaki and Murao, 2000; Yamaguchi and Yamazaki, 2000; Bommer et al., 2002), but the Indian and Nepalese curves may be the most suitable for Bangladeshi structures, until Bangladeshi researchers develop their own fragility curves. In this study, fragility curves for the buildings in Dhaka were prepared by calibrating the existing fragility curves for Indian buildings prepared by Arya (2000) and for Nepalese buildings prepared by Bothara et al. (2000). Neither Arya (2000) nor Bothara et al. (2000) mentioned the types of damages (i.e., collapsed or heavily or moderately damaged) to be estimated using those fragility curves. Segawa et al. (2002) used those curves after some calibration and quoted them to be developed for heavily damaged structures.

7.2. Human casualty distributions. In order to assess the human casualty levels due to the earthquake, the estimates of average fatality and injury levels have been used. These Figures have been derived by using a mortality prediction model for different categories of structures. This prediction model is based on investigation of casualty due to several major earthquakes that have occurred during the last century (Coburn et al., 1992).

7.3. Analysis method for seismic damage estimation of gas pipeline and water pipeline. Quantitative studies on seismic damage for gas and water supply pipelines in Bangladesh are not available. Although the strength of the pipeline materials is not particularly different from that of the pipeline materials in other countries, it is considered that the construction quality of the joints always leads to problems. Damage of gas pipeline system and water supply system of Bangladesh are assessed base on some recent damage functions developed for different gas line systems during Chi-Chi (or called Ji-Ji) earthquake in Taiwan (2002). In order to perform analysis, the study area is divided into 1 km × 1 km grid with pipelines enclosed in the grid, and the damage locations. For each group of pipelines, the damage ratio (DR) that is also denoted as the repair rate (RR) was calculated by dividing the numbers of damage by the total length of gas pipelines in each grid. All these damage ratio (DR) relations are functions of PGA and pipe diameter (Chen et al., 2002) and which were similar to that, obtained in the Northridge earthquake by Toprak (1998).

8. Loss assessment

From attenuation law, peak ground acceleration in the bedrock level is estimated and is used to develop a regional combined seismic hazard map based on site amplification, liquefaction and landslide. These hazard maps are then overlaid and combined with the structural inventory maps, and water and gas supply system maps to produce maps of regional damage distributions. Combining the map of damage distributions with a map of population distributions for the area results in final regional estimates of direct monetary loss such as buildings, water and gas supply systems and non-monetary loss such as fatalities and injuries. The method to combine the

different hazards is based on weighted average approach. For human casualty estimation a morbidity model suggested by Coburn et al. (1992) was used. Finally economic loss estimation was estimated using the damages expected to be suffered due to the scenario event. Table 4 provides an overview of the most significant losses that would be sustained in Sylhet due to recurrence of Srimangal earthquake (1918).

Table 4. Overview of results for key parameters in the case of 8 July 1918 Srimangal earthquake (M = 7.6) scenarios

Category	Description of parameters	Results
Hazards	Peak ground acceleration (PGA)	Maximum 1.56g Minimum 0.35g
Lifelines	Damage to potable water pipes	Total number of damaged points 204 (total affected length 118.53 km). This covers both analysis 1 and 2.
	Treatment plant with at least moderate damage	Has not been conducted separately.
	Damage natural gas supply pipes	Total number of damaged points 981 (total affected length 436 km).
Building damage	Total number of buildings damaged A type B1 type B2 type C type D type F type	15320 59% 76% 76% 55% 12% 15%
Casualties	Morning event: injuries Deaths	20569 (6.6% of total population) 17249 (5.5% of total population)
	Noon event: injuries Deaths	13979 (4.5% of total population) 11713 (3.75% of total population)
	Night event: injuries Deaths	25875 (8.3% of total population) 21674 (7% of total population)

The findings highlight several critical factors that have important implications for earthquake risk reduction, planning, preparedness, emergency response, and disaster recovery. Results indicate, that the M = 7.6 Srimangal scenario would be the most destructive and disruptive to the Sylhet City. Results from the M = 7.6 scenario include the following:

- 65% area will be affected with intensity 10, 28% area will be affected with intensity 9, 5.5% area will be affected with intensity 8, and 1.5% area will be affected with intensity 11.
- A nighttime event will cause the highest number of casualties (Figure 20). Of the estimated 47549 (approximately 15% of total population) casualties, close to 25875 or about 54 percent will be major injuries (injuries requiring hospitalization) or fatalities (about 21674).
- Nearly 15320 buildings are expected to be damaged.

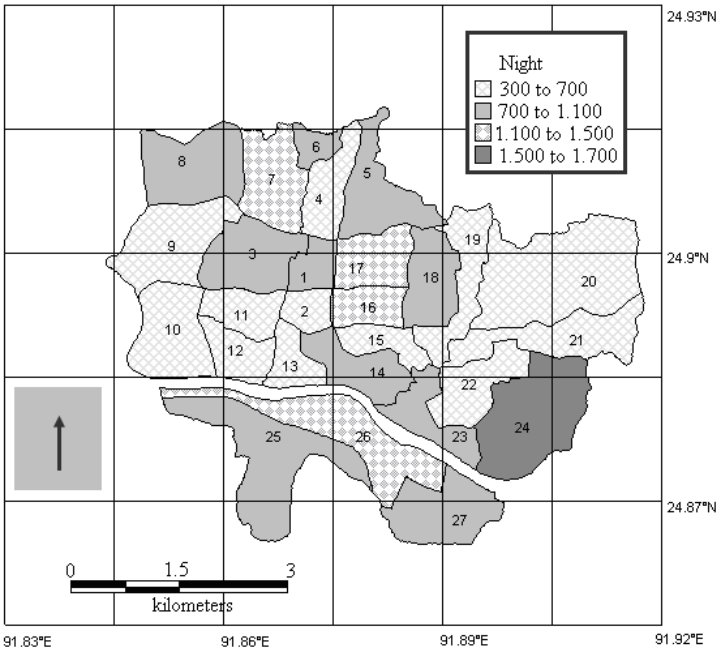

Fig. 20. Map showing total number of deaths at night in Sylhet City

- There could be safety issues related to school children, teachers, and other persons in school buildings. The catastrophic failure or partial collapse of one or more school buildings during school periods could greatly increase the casualty estimates. Restoration of the schools for the emergency sheltering of the homeless and other contingency service will be demanding.
- Schools and fire stations are particularly vulnerable to damage. These losses are due to insufficient seismic building code standards and the vintage of the building stock, the majority of the structures in the city. This situation may lead to issues with respect to providing reliable shelters for immediate use in emergency response and sheltering.
- Hospitals might suffer significant building damage. Due to hospital damage the city may face the serious issue of how to provide the needed care to existing patients and potentially thousands of earthquake victims from the affected communities.
- A good portion of the Sylhet City is susceptible to liquefaction. Ground failure effects, on the other hand, are more significant in the Charleston area for pipelines, roads and runways.
- Few million tons of debris will be generated, which includes concrete and steel-materials that require special treatment in "deconstruction" and disposal. Debris disposal, therefore, may pose a major challenge in the recovery phase. This total does not include biomass.
- In potable water pipes total number of damage points estimated 204 and total affected length 118.53 km. Widespread water failure may drain water within minutes or hours from the distribution system, thus preventing adequate water supply for fire suppression. In addition, rest of the urban households in the affected area will be deprived of water. It will take weeks, if not months, to restore the serviceability of the water systems. Therefore, significant external augmentation would be required to provide and sustain such a high repair level.
- Of all the utility systems, gas supply system is arguably the most critical for Bangladesh, as the natural gas is being used by the households as well as in many power plants. In natural gas supply system total number of damaged points estimated 981 and total affected length 436 km.
- This study is carried out only at Sylhet City Corporation area, which occupies 26.50 km^2, where Sylhet Sadar Upazilla occupies 517.43 km^2. It is believed that if potential earthquake trigger in northeastern part of Bangladesh, not only Sylhet City Corporation but also other parts of this Upazilla might be severally affected. Consequently, if loss estimation is done according to above mentioned issues, it is very realistic that total loss due to this scenario event might exceed several billion US dollars, which is also be interpolated from past earthquake such as is September 21, 1999, in Taiwan city. This earthquake caused at least 2,297 deaths, 8700 injuries, left 600,000 people homeless, and damaged about 82,000 housing units.

Conclusions and authors' perspective

This study proposes a methodology for seismic risk assessment of Sylhet, Bangladesh. This paper provides post-earthquake assessment and helps to disaster management for Bangladesh. In this study, a scenario event of 1918 Srimangal earthquake of magnitude M = 7.6 was considered and microzonation maps were produced. 2071 borehole data were used for this purpose of which 9 were 30 m deep and remaining were 15 to 20 m deep. This can be verified by carrying out more borehole data in future.

A repeat of the 1918 Srimangal earthquake may cause the City to be overwhelmed by widespread damage as well as the disruption of lifelines. The picture for Sylhet is particularly severe.

Fires may spread unfought since water pipeline ruptures will inhibit suppression. Damage to emergency services including police, fire, and hospitals, will be extensive. Access by bridges may be hampered (though the vulnerability of Surma and other bridges has not been studied separately).

The impact of this event demonstrates the scope of the problem and reinforces the need to implement structural and non-structural mitigation measures as a central feature in long-term initiatives to reduce seismic risk. Affected communities will be coping with the trauma and demands of immediate response and early recovery. Early government assistance, along with first-tier support drawn from the non-affected regions, will be of highest priority. Still, a well-coordinated, preplanned response involving all levels of government, along with the private sector and other groups, will be required to deal effectively with the consequences of an event of this magnitude. Establishing centralized communications, command, and control to coordinate rescue efforts will be immediately critical. Transporting the injured to hospitals will require priority action. Directing fire-fighting efforts to the most essential facilities and to control the spread of fires will require prompt action to minimize casualties and property loss. The emergency inspection and repair of minimum critical water pipeline segments must be well fo-

cused in coordination with the fire department. Directing debris removal may require priority for passage of emergency vehicles.

By characterizing the nature and scope of potential impacts, the study performed for Sylhet City represents a starting point for renewed and hopefully more effective efforts in earthquake hazard and loss mitigation. From this study, many in the City as well as in the Country now well understand that a very significant earthquake hazard exists in Sylhet. During the past few years, a lot of seminar and symposium have been arranged in government and non-government levels for public awareness and for earthquake emergency response plans. This study will be helpful for the planners and decision makers.

References

1. Applied Technology Council (1985). Earthquake Losses Evaluation Methodology and Databases for Utah, ATC-36, Redwood City, California.
2. Arya, A. (2000). Non-engineered construction in developing countries: an approach toward earthquake risk prediction, Proc. of 12th WCEE, No. 2824.
3. Bangladesh Petroleum Exploration and Production Company Limited (BAPEX) (1989). International Report on the Kailas Tila Structure.
4. Bangladesh Bureau of Statistics (BBS) (1996). Population Census Report, 1991, Dhaka.
5. Bilham R., Gaur V.K., Molnar P. (2001). Himalayan Seismic Hazard, Science, Vol. 293.
6. BNBC (1993). Bangladesh National Building Code, HBRI-BSTI.
7. Bommer, J.R. Spance, M. Erdik, S. Tabuchi, N. Aydinoglu, E. Booth, D.del Re and O. Peterken (2002). Development of an earthquake loss model for Turkish catastrophe insurance, *Journal of Seismology*, Volume 6.
8. Boore D., Joyner W., Fumal T.E. (1997). Equation for estimating horizontal response spectra and peak acceleration from Western North American Earthquakes: a summary of recent work, Seism. Res. Lett., Vol. 68, No.1, pp 128-153.
9. Brunschweiller R.O. (1980). Lithographic monsters in modern oil exploration, Proc. Offshore South-East Asia Conf., Singapore.
10. OYO Corporation International (OIC) (2009). Unpublished report on earthquake sources within Bangladesh.
11. Chen, W.W., B. Shih, Y. Chen, J.H. Hung, H.H. Hwang (2002). Seismic Response of Natural Gas and Water Pipelines in the Ji-Ji Earthquake, Soil Dynamics and Earthquake Engineering, Vol. 22, pp.1209-1214.
12. Coburn A.W., Spence R.J.S. and Pomonis A. (1992). Factors Determining Human Casualty Levels in Earthquakes: Mortality Prediction in Building Collapse, Proceedings of the 10th World Conference on Earthquake Engineering, Madrid, Spain, Vol. 10, pp. 5989-5994.
13. Coleman J.M. (1969). Brahmaputra river-channel processes and sedimentation: sedimentary geology, Vol.3 2/3, pp. 131-239.
14. Geological Survey of Bangladesh (GSB) (1990). Geological map of Bangladesh.
15. Grunthal G, editor (1998). European Macroseismic Scale, Luxembourg: Cahiers due Centre European de Geodynamique et de Seismologie, Vol. 15.
16. Hasen, A. and C.A.M. Franks (1991). Characteristic and Mapping of Earthquake Triggered Landslides for Seismic Zonation, Stanford, California, August 25-29, 1991. Vol. 1, pp. 149-195.
17. Hiller K. and Elahi M. (1988). Structural growth and hydrocarbon entrapment in the Surma Basin, Bangladesh, In Wagner et al., (Eds), Petroleum Resources of China and Related Subjects, Earth Sci. Series, Vol. 10, pp 657-669.
18. Iwasaki T., K. Tokida, F. Tatsuoka, S. Watanabe, S. Yasuda, and H. Sato (1982). Microzonation for Soil Liquefaction Using Simplified Methods, Proceedings of the Third International Earthquake Microzonation Conference. Seattle, Washington. Vol. 3, pp. 1319-1330.
19. Johnson S.Y. and Alam A.M.N. (1991). Sedimentation and tectonics of the Sylhet Trough, Bangladesh, Bull. Geol. Soc. Am., Vol. 103, pp. 1513-1522.
20. Juang C.H. and Elton D.J. (1991). Use of Fuzzy Sets for Liquefaction Susceptibility Zonation, Proceedings of the Fourth International Conference on Seismic Zonation, Stanford California, August 25-29, 1991, Vol. 2, pp. 629-636.
21. Kircher, C.A, A.A. Nassar, O. Kustu and W.T. Holmes (1997). Development of building damage functions for earthquake estimation, Earthquake Spectra, Vol. 13 (4).
22. Kiremidjian, A.S. (1992). Methods for regional damage estimation, Proceedings of the 10th World's Conference on Earthquake Engineering, Madrid, Spain, July 19-24, 1992.
23. Kiremidjian, A.S., S.A. King, M. Sugito, and H.C. Shah (1991). Simple Site Dependent Ground Motion Parameters for the San Francisco Bay Region, The John A Blume Earthquake Engineering Center Report, No. 97, Department of Civil Engineering, Stanford University, Stanford, California.
24. Korkmaz, A.K. (2009). Earthquake disaster risk assessment and evaluation for Turkey, Environ. Geol., 57, pp. 307-320.
25. McGuire, R. (1978). Seismic ground motion parameters relations, Journal of Geotechnical Division, ASCE, Vol. 104, pp. 461-490.
26. Molnar, P., and Tapponier, P. (1975). Cenozoic tectonics of Asia, effects of a continental collision, Science, Vol. 189 (8), pp. 419-426.
27. Reitherman, R. (1985). A Review of Earthquake Damage Estimation Methods, Earthquake Spectra, Vol. 1, No 4, pp. 805-847.

28. Rojahn, C. (1993). Estimation of Earthquake Damage to Buildings and Other Structures in Large Urban Areas. Proceedings of the Geohazards International/Oyo Pacific Workshop, Istanbul, Turkey, October 8-11, 1993.
29. Sabri S.A. (2001). Earthquake intensity-attenuation relationship for Bangladesh and its surrounding region, M. Engg, Thesis, BUET, Dhaka-1000.
30. Schnabel P.B., Lysmer J., Seed H.B. (1972). SHAKE – a Computer Program for Earthquake Response Analysis of Horizontally Layered Sites, Earthquake Engineering Research Centre Report 72-12, University of California, Berkeley, USA.
31. Schneider P. and Schauer B. (2005). An earthquake risk assessment tool for Turkey, HAZTURK strategies for earthquake loss estimation program for Turkey, Istanbul.
32. Seed, H.B., I.M. Idriss (1971). Simplified Procedure for Evaluating Liquefaction Potential, *ASCE Journal of the Soil Mechanics and Foundation Division*, Volume SM9, pp. 1249-1273.
33. Sharfuddin M. (2001). Earthquake Hazard Analysis for Bangladesh, M.Sc. Engg, Thesis, BUET, Dhaka-1000.
34. Stuart M. (1920). The Srimangal earthquake of 8th July 1918, Memoir of Geological Survey of India, Vol. 46, pp.1-70.
35. Sylhet City Corporation (1998). Sylhet City Plan.
36. Talukder S, Islam M.S. and Islam M.A. (2006). Seismic Stratigraphy of the Kailas Tila Structure, Sylhet Trough, Bangladesh, *Bangladesh Journal of Geology*, Vol. 25, pp. 31-47.
37. Tamura I. and Yamazaki F. (2002). Estimation of S-wave velocity based on geological survey data for K-NET and Yokohama seismometer network, *Journal of Structural Mechanics and Earthquake Engineering* No. 696, Vol. 1(58), pp. 237-248 (in Japanese).
38. Toprak S. (1998). Earthquake effects on buried lifeline systems, Ph.D. Dissertation, Cornell University.
39. Trifunac M.D., Brady (1975). Preliminary Analysis of the Peaks of Earthquake Strong Ground Motion-Dependence of Earthquake Peaks on Earthquake Magnitude, Epicentral Distance, and Recording Site Conditions. Bulletin of the Seismological Society of American, Vol. 1, pp 139-162.
40. Wieczorek, G.F., R.C. Wilson, and E.L. Harp (1985). Map Showing Slope Stability During Earthquake in San Mateo Country California, Map-I-1257-E, United States Geological Survey, Menlo Park, California.
41. Wilson R.C. and D.K. Keefer (1985). Predicting Areal Limits of Earthquake Induced Landsliding, Evaluating Earthquake Hazards in the Los Angeles Region, Professional Paper, 1360, United States Geological Survey, Pasadena, California, pp 317-493.
42. Youd T.L. (1991). Mapping of Earthquake-Induced Liquefaction for Seismic Zonation, Proceedings of the Fourth International Conference on Seismic Zonation, Stanford, California, August 25-29, 1991, Vol. 1, pp. 111-147.